

DYNAMICS AND BIFURCATIONS OF A 3D SYSTEM
MODELING THERMAL INSTABILITY

MIAOHUA JIANG
INSTITUTE FOR MATHEMATICS AND ITS APPLICATIONS
514 VINCENT HALL, 206 CHURCH STREET SE
UNIVERSITY OF MINNESOTA
MINNEAPOLIS, MN 55455

ABSTRACT. We study the dynamics of a 3D dynamical system modeling thermal instability in solid combustion and give a complete classification of its Hopf bifurcation with respect to two parameters in the kinetic function. We show that the system does not have a Siniukov-Hopf bifurcation contrary to the seemingly apparent infinite period bifurcation.

1. INTRODUCTION

In [1] and [5], the authors introduced a 3D dynamical system (given in next section) modeling the temperature dynamics in solid combustion. The system was obtained by applying a pseudo-spectral approximation to the following one-phase free boundary problem formulated by the same authors in their earlier works [2], [3], and [4]:

$$(1) \quad \begin{aligned} u_t &= u_{zz}, \quad z < S(t), \quad S(0) = 0; \\ u(z, 0) &= u_0(z), \quad z \leq 0, \quad u_0(z) \geq 0; \\ u(S(t), t) &= 1 + \mu K(-V(t)), \quad t > 0, \quad V(t) = \frac{dS}{dt}; \\ u_x(S(t), t) &= -V(t), \quad t > 0. \end{aligned}$$

Numerical results in both papers [1] and [5] shown that in certain parameter region, the 3D system possesses interesting solutions with periodic burstings that closely resembles the dynamics of the original free boundary problem (1). It was suggested that there exists possibly a homoclinic orbit at the equilibrium while the system is at its subcritical Hopf-bifurcation point.

Date: July, 1998.

1991 Mathematics Subject Classification. 34, 58.

Key words and phrases. Siniukov orbit, Hopf bifurcation, thermal instability .

In this technical report, we combine the normal form reduction at the equilibrium point and numerical simulations of the system to study further its dynamics and bifurcations. We obtain a complete classification of the Hopf bifurcation point according to whether it is supercritical or subcritical with respect to two parameters in the kinetic function $K(-V)$. Then, with numerical simulation, we show that there is no homoclinic orbit at the equilibrium.

We skip the derivation of the 3D system since it is presented in both papers [1] and [5] in detail. The normal form reduction is performed with help of Mathematica and the numerical simulation is done with DSTOOL (tcl/tk version). The problem was suggested to the author by John Guckenheimer.

2. NORMAL FORM AND CLASSIFICATION OF HOPF BIFURCATION

In this section, we perform the normal form reduction to the system below to obtain Hopf bifurcation diagram with respect to two parameters in the kinetic function.

2.1. The dynamical system. The system is directly obtained from [1].

$$(2) \quad \begin{aligned} \dot{x} &= 3[-2x - 3y - \frac{h}{2} + \frac{\mu k}{2}(v+1) + v^2 - vx] + 3y(v+1) + vx, \\ \dot{y} &= -2x - 3y - \frac{h}{2} + \frac{\mu k}{2}(v+1) + v^2 - vx + vy, \\ \dot{v} &= h, \end{aligned}$$

where

$$h = \frac{(2x - \mu k - v^2)}{\mu k'}$$

and $k = k(v)$ is the normalized kinetic function with $k(0) = 0, k'(0) = -1$.

The relations between the variables in this system and the original PDE system (1) are

$$v = 1 + V(t), \quad k(v) = K(1 - v);$$

$x(t), y(t)$ are related to the approximate deviation of the solution from the basic traveling-wave solution $u(z, t) = e^{z+it}$.

2.2. The normal form. The origin $(x, y, v) = (0, 0, 0)$ is an equilibrium point for all values of the parameter μ . Linearizing around this equilibrium point, we obtain three eigenvalues:

$$\lambda_1 = -1, \quad \lambda_{2,3} = \frac{1}{2}(9 - 3/\mu \pm \sqrt{(9 - 3/\mu)^2 - 12}).$$

The value $\mu = 1/3$ is a Hopf bifurcation point. We classify this Hopf bifurcation point according to whether it is supercritical or subcritical. The kinetic function $k(v)$ is assumed to be smooth. Since we need only to consider at most cubic terms in the expansion of the vector field around the equilibrium, we take the most general form for $k(v)$:

$$k(v) = -v + \alpha v^2 + b v^3.$$

Plug $k(v)$ into the system and truncate it to obtain the following system.

$$(3) \quad \begin{aligned} \dot{x} &= \frac{1}{2\mu} \left(3\mu^2 v (-1 + (-1 + \alpha) v + (\alpha + b) v^2) \right. \\ &\quad + 3 (-2\alpha v^3 + 2x + 4avx + v^2 (-1 + 8\alpha^2 x + 6bx)) \\ &\quad \left. + \mu (3(2 + \alpha) v^2 + 6(\alpha^2 + b) v^3 - 12(x + y) + v(3 - 4x + 6y)) \right), \\ \dot{y} &= \frac{1}{2\mu} \left(-2\alpha v^3 + \mu^2 v (-1 + (-1 + \alpha) v + (\alpha + b) v^2) + 2x + 4avx \right. \\ &\quad \left. + v^2 (-1 + 8\alpha^2 x + 6bx) + \mu ((2 + \alpha) v^2 + 2(\alpha^2 + b) v^3 - 4x - 6y + v(1 - 2x + 2y)) \right), \\ \dot{v} &= \frac{1}{2\mu} \left(2\alpha v^3 - \mu v (1 + \alpha v + 2\alpha^2 v^2 + 2bv^2) - 2x - 4avx + v^2 (1 - 8\alpha^2 x - 6bx) \right). \end{aligned}$$

We first make a linear transformation to the truncated system using vectors in the corresponding eigenspaces as a basis.

$$(4) \quad \begin{aligned} x &= (1/4)(7\mu - 3)u - (1/4)l^{1/2}w, \\ y &= (1/4)(1 - \mu)s + (1/4)(3\mu - 1)u - (1/12)l^{1/2}w, \\ v &= s + u, \end{aligned}$$

where $l = 54\mu - 69\mu^2 - 9$.

At the Hopf bifurcation point $\mu = 1/3$, we have the system in terms of (s, u, w) .

$$\begin{aligned}
(5) \quad \dot{s} &= -s + \frac{1}{2} \left(2(-3\alpha + \alpha^2 + b) s^3 + s^2 \left(-3 + \alpha - 18\alpha u + 36u - 3\sqrt{3}bw + 2\alpha^2 (u - 2\sqrt{3}w) \right) \right. \\
&\quad \left. - u \left((6\alpha + 2\alpha^2 + b) u^2 + \sqrt{3}(-1 + 2\alpha) w + u \left(2 + \alpha + 4\sqrt{3}\alpha^2 w + 3\sqrt{3}bw \right) \right) \right. \\
&\quad \left. - s \left(2\alpha(9 + \alpha) u^2 - \sqrt{3}w + 2\sqrt{3}\alpha w + u \left(5 + 8\sqrt{3}\alpha^2 w + 6\sqrt{3}bw \right) \right) \right) \\
\dot{u} &= \sqrt{3}w + \frac{1}{2} \left(-6(-3\alpha + \alpha^2 + b) s^3 + 3(6\alpha + 2\alpha^2 + b) u^3 + \sqrt{3}(-1 + 6\alpha) uw \right. \\
&\quad \left. + u^2 \left(8 + 3\alpha + 3\sqrt{3}(4\alpha^2 + 3b)w \right) - 3s^2 \left(\alpha - 3 + (2\alpha^2 - 18\alpha + 3b)u - \sqrt{3}(3b + 4\alpha^2)w + \right. \right. \\
&\quad \left. \left. + s \left(6\alpha(9 + \alpha) u^2 + \sqrt{3}(-1 + 6\alpha) w + u \left(17 + 24\sqrt{3}\alpha^2 w + 18\sqrt{3}bw \right) \right) \right) \right) \\
\dot{w} &= -\sqrt{3}u \\
&\quad + \frac{1}{2\sqrt{3}} \left(6(14\alpha - 5\alpha^2 - 6b) s^3 + s^2 \left(9 - 21\alpha + (252\alpha - 30\alpha^2 - 63b)u + 15\sqrt{3}(4\alpha^2 + 3b)w \right) \right. \\
&\quad \left. + u \left(-6 + 3(28\alpha + 10\alpha^2 + 3b) u^2 - \sqrt{3}w + 30\sqrt{3}\alpha w + 3u \left(4 + 3\alpha + 20\sqrt{3}\alpha^2 w + 15\sqrt{3}bw \right) \right) \right. \\
&\quad \left. + s \left(6(42\alpha + 5\alpha^2 - 3b) u^2 + \sqrt{3}(-1 + 30\alpha) w + 3u \left(7 - 4\alpha + 40\sqrt{3}\alpha^2 w + 30\sqrt{3}bw \right) \right) \right)
\end{aligned}$$

According to the normal form theory [GH], we can find a quadratic transformation that eliminates all quadratic terms in the expression of the vector field (5):

$$\begin{aligned}
(6) \quad s &= p + \frac{(3-\alpha)p^2}{2} - \frac{(11+13\alpha)q^2}{26} + \frac{5\sqrt{3}qr}{26} - \frac{15r^2}{26} + p \left(\frac{(3-6\alpha)q}{6} + \frac{5r}{2\sqrt{3}} \right) \\
u &= q - \frac{3(3+5\alpha)p^2}{14} + \frac{(1+3\alpha)q^2}{2} + \frac{3r^2}{2} - \left(\frac{5}{2\sqrt{3}} + 2\sqrt{3}\alpha \right) qr \\
&\quad - \frac{p}{26} \left((95+174\alpha)q + \sqrt{3}(36\alpha-31)r \right) \\
w &= r + \frac{\sqrt{3}(-15+17\alpha)p^2}{14} + \frac{\sqrt{3}(-1+3\alpha)q^2}{2} - \frac{3qr}{2} - \left(\frac{-5}{2\sqrt{3}} + 2\sqrt{3}\alpha \right) r^2 \\
&\quad + \frac{p}{26} \left(\sqrt{3}(-73+94\alpha)q - (113+216\alpha)r \right)
\end{aligned}$$

The new system in variables (p, q, r) is given next. We retain only the terms of orders less than or equal to three.

$$\begin{aligned}
(7) \quad \dot{p} &= -p + \frac{1}{546} \left(-39(63 - 108a + 44a^2 - 14b)p^3 + p^2(-3(118 - 6215a + 2442a^2 - 273b)q \right. \\
&\quad \left. + \sqrt{3}(-3945 + 1553a + 4302a^2 - 8196)r) - 21p \left((-29 - 662a + 264a^2)q^2 + 2\sqrt{3}(97 \right. \right. \\
&\quad \left. \left. - 101a - 174a^2 + 396)qr + (6 + 240a - 264a^2)r^2) - 7(3(18 + 39a + 182a^2 + 136)q^3 \right. \right. \\
&\quad \left. \left. - \sqrt{3}(37 + 527a - 78a^2 - 117b)q^2r + 6(49 + 40a - 156a^2)qr^2 - 36\sqrt{3}(1 - 2a)r^3) \right) \\
\dot{q} &= \sqrt{3}r + \frac{1}{546} \left(117(45 - 96a + 44a^2 - 14b)p^3 + 3p^2 \left((-2390 - 17707a + 7326a^2 - 8196)q \right. \right. \\
&\quad \left. \left. + \sqrt{3}(3527 - 3603a - 4302a^2 + 8196)r) + 21p \left((-509 - 1922a + 792a^2)q^2 + 2\sqrt{3}(205 \right. \right. \\
&\quad \left. \left. - 573a - 522a^2 + 117b)qr + 6(25 + 76a - 132a^2)r^2) + 7(3(30 + 299a + 546a^2 + 396)q^3 \right. \right. \\
&\quad \left. \left. - \sqrt{3}(337 + 1815a - 234a^2 - 351b)q^2r + 6(121 - 36a - 468a^2)qr^2 - 36\sqrt{3}(1 - 6a)r^3) \right) \\
\dot{r} &= -\sqrt{3}q + \frac{1}{546} \left(117\sqrt{3}(13 - 80a + 88a^2 - 28b)p^3 + 3p^2 \left(\sqrt{3}(-1214 - 9497a + 15582a^2 \right. \right. \\
&\quad \left. \left. - 19116)q + (3961 - 15759a - 19998a^2 + 40956)r) + 21p \left(\sqrt{3}(-279 - 1214a \right. \right. \right. \\
&\quad \left. \left. + 1668a^2 - 78b)q^2 + 2(267 - 2053a - 2346a^2 + 5856)qr + 4\sqrt{3}(19 + 134a - 330a^2)r^2) \right. \right. \\
&\quad \left. \left. + 7 \left(3\sqrt{3}(20 + 321a + 858a^2 + 396)q^3 + 3(-189 - 1417a + 702a^2 + 5856)q^2r \right. \right. \right. \\
&\quad \left. \left. + 36(-1 + 30a)r^3 + 2\sqrt{3}(184 - 564a - 2340a^2)qr^2) \right) \right)
\end{aligned}$$

To determine the type of Hopf bifurcations, we need to restrict the vector field to a central manifold corresponding to the pair of imaginary eigenvalues. However, since any central manifold is tangent to the plane $p = 0$ at the origin, the equation for the central manifold can be written as $p = p(q, r)$, where $p(q, r)$ is at least of order 2 in terms of q, r (in fact, order 3 in this case, since there is no quadratic terms) near the equilibrium. Substitute $p(q, r)$ for p into the last two equations in the system. We see that all terms containing $p(q, r)$ will be

at least of order 4 and therefore, we can simply set $p = 0$ to obtain the following system.

(8)

$$\begin{aligned} \dot{q} &= \sqrt{3}r + \frac{1}{78} \left(3(30 + 299a + 546a^2 + 396)q^3 - \sqrt{3}(337 + 1815a - 234a^2 - 3516)q^2r \right. \\ &\quad \left. - 6(-121 + 36a + 468a^2)qr^2 + 36\sqrt{3}(-1 + 6a)r^3 \right) \\ \dot{r} &= -\sqrt{3}q + \frac{1}{78} \left(3\sqrt{3}(20 + 321a + 858a^2 + 396)q^3 - 3(189 + 1417a - 702a^2 - 5856)q^2r \right. \\ &\quad \left. + 36(-1 + 30a)r^3 - 8\sqrt{3}(-46 + 141a + 585a^2)qr^2 \right) \end{aligned}$$

The normal form theory [GH] again tells us that we can further apply a cubic transformation to obtain the normal form in the center manifold. The explicit formula of cubic transformation is omitted because it is rather long. The normal form is given in variables (X, Y) .

(9)

$$\begin{aligned} \dot{X} &= \sqrt{3}Y + \frac{1}{208} \left((107 + 488a + 1404a^2 + 702b)X^3 - \sqrt{3}(331 + 976a + 936a^2)X^2Y \right. \\ &\quad \left. + (107 + 488a + 1404a^2 + 702b)XY^2 - \sqrt{3}((331 + 976a + 936a^2)Y^3) \right) \\ \dot{Y} &= -\sqrt{3}X + \frac{1}{208} \left(\sqrt{3}(331 + 976a + 936a^2)X^3 + (107 + 488a + 1404a^2 + 702b)X^2Y \right. \\ &\quad \left. + (107 + 488a + 1404a^2 + 702b)Y^3 + \sqrt{3}((331 + 976a + 936a^2)XY^2) \right). \end{aligned}$$

Thus, the type of Hopf bifurcation is determined by the sign of the coefficient

$$c = \frac{1}{208} (107 + 488a + 1404a^2 + 702b).$$

If $c < 0$, the Hopf bifurcation point $\mu = 1/3$ is supercritical and if $c > 0$, the Hopf bifurcation is subcritical. In terms of parameters a, b , if $b < -22673/246402 \approx -0.092$, the Hopf bifurcation point $\mu = 1/3$ is supercritical when a is in the interval

$$I = \left(\frac{-122 - \sqrt{-22673 - 246402b}}{702}, \frac{-122 + \sqrt{-22673 - 246402b}}{702} \right);$$

the Hopf bifurcation is subcritical when $a \notin I$ excluding the endpoints. For $b > -22673/246402$, the Hopf bifurcation is subcritical for all values of a .

2.3. Two Examples. There are two types of kinetic functions considered in this model [5] [10]. The first kind is Arrhenius-type kinetics obtained from modifying kinetics in gas

combustion [10];

$$k_1(v) = \frac{\log(1-v)}{1-\gamma\log(1-v)}.$$

The second type was introduced in [5] for numerical simulation, which resembles $k_1(v)$ around $v = 0$.

$$k_2(v) = \frac{(1-v)^\alpha - (1-v)^{-\beta}}{\alpha + \beta}.$$

Expand both functions into power series around $v = 0$. We have

(10)

$$k_1(v) = -v + \left(-\frac{1}{2} + \gamma\right)v^2 + \left(-\frac{1}{3} + \gamma - \gamma^2\right)v^3 + O(v^4).$$

(11)

$$k_2(v) = -v + \frac{-1 + \alpha - \beta}{2}v^2 + \frac{-2 + 3\alpha - \alpha^2 - 3\beta + \alpha\beta - \beta^2}{6}v^3 + O(v^4).$$

For the first type of kinetic function k_1 , we have

$$c = \frac{1}{104}(-10 - 107\gamma + 351\gamma^2).$$

Thus, the Hopf bifurcation is supercritical if

$$\gamma \in (-0.075, 0.38).$$

For the kinetic function k_2 ,

$$c = -20 + 234\alpha^2 + 107\beta + 234\beta^2 - \alpha(107 + 585\beta).$$

The condition to be supercritical for the Hopf bifurcation point $c < 0$ is then equivalent to

$$|468\alpha - 107 - 585\beta| < \sqrt{30169 + 25038\alpha + 123201\beta^2}.$$

When $\beta = 1$, the interval where Hopf bifurcation is supercritical is $\alpha \in (0.5761, 2.381162)$, whose approximate value was found numerically in [1].

3. SEARCHING FOR A ŠILNIKOV ORBIT

For the second kind of kinetic function k_2 , in both PDE case and its finite-dimensional approximate ODE system, it is shown numerically that there apparently exists an infinite period bifurcation, which indicates the possible existence of a homoclinic orbit at the Hopf bifurcation point in the subcritical region. This coincidence of existence of a homoclinic orbit at a subcritical Hopf bifurcation is also called Šilnikov-Hopf bifurcation [11][14].

3.1. Silnikov-Hopf bifurcation. The normal form reduction will enable us to further investigate this phenomenon numerically. We first state a result concerning the consequences of the existence of such orbit.

[8] *If $\mu = 1/3, (\alpha, \beta) = (\alpha_0, \beta_0)$ is a subcritical Hopf bifurcation point and there exists a homoclinic orbit at the equilibrium point, then, there exists a curve Γ in the parameter space (μ, α) , $\mu < 1/3$ (with $\beta = \beta_0$ fixed) starting from the point $(1/3, \alpha_0)$ such that the system is hyperbolic and possesses a homoclinic orbit for all $(\mu, \alpha) \in \Gamma$.*

This result follows from part (a) of the main theorem in [8]. The curve Γ is defined by zeros of the Melnikov function, which measures the distance between the orbit in the stable manifold and the unstable manifold of the equilibrium. Using this result we now describe a strategy of verifying the existence of Silnikov-Hopf bifurcation.

Assume that for parameters μ_0, α_0, β_0 , the system has a homoclinic orbit at the equilibrium, where $\mu_0 \in (1/3 - \delta, 1/3]$ with $\delta > 0$ small. When $\mu_0 = 1/3$, the parameters (α_0, β_0) are necessarily in the region D where the Hopf bifurcation is subcritical. When $\mu_0 < 1/3$, by the continuity, the parameters (α_0, β_0) are in a small neighborhood of this region D .

We shall use the system in variables (s, u, w) , i.e., the linearly transformed one. In this coordinate system, the stable manifold is tangent to the s -axis and the unstable (central) manifold is tangent to the plane $s = 0$. Now, we select a rectangular domain near the origin:

$$\Sigma = \{(s, u, w) \mid -\epsilon \leq s \leq \epsilon, 0 < \rho_1 \leq u \leq \rho_2 < 1, w = 0\}.$$

We can choose ϵ and ρ_1, ρ_2 such that the homoclinic orbit passes Σ transversally if it ever exists. The guidelines of choices are:

1. The rectangle Σ should be small since we will look for homoclinic orbit passing Σ .
2. To choose ρ_1, ρ_2 , we need to make sure that the interval $[\rho_1, \rho_2]$ is long enough so that when the homoclinic orbit spirals out, its projection to the $s = 0$ plane will intersect this interval. We consider the linear approximation of the vector field in the unstable manifold in the polar coordinates:

$$\dot{\rho} = c\rho, \quad \dot{\theta} = \omega.$$

The condition $\rho_2 > \rho_1(1 + c\frac{2\pi}{\omega})$ will guarantee that the spiraling-out orbit intersects the interval.

3. Since the equation for the unstable manifold is of order two near the origin, the ϵ can be chosen at the scale of $C\rho_2^2$, where C depends on the nonlinear part of the first equation of (5).

For, any parameters μ, α, β , if there exists a homoclinic orbit at the equilibrium, then, there exists an orbit $\phi(t) = (s(t), u(t), w(t))$, $0 \leq t < \infty$ with $\phi(0) \in \Sigma$ and

$$(12) \quad \lim_{t \rightarrow \infty} \|\phi(t)\|^2 = \lim_{t \rightarrow \infty} s^2(t) + u^2(t) + w^2(t) = 0.$$

Note that this is only a necessary condition. The condition becomes sufficient if we require that $\phi(0)$ be in the unstable manifold.

For the system (5), we show numerically that the condition (12) does not hold for any μ close to $1/3$ and any parameters (α, β) in the neighborhood of D . Our numerical results show that

$$(13) \quad \min_{\mu} \min_{(\alpha, \beta) \in D} \min_{t \geq 0} u^2(t) + w^2(t) \approx 0.01.$$

3.2. Remarks.

1. *Increasing length of periods:* It is shown in [1] that, as $\mu \rightarrow 1/3$, there are periodic orbits with longer and longer periods, which indicates the possible existence of a homoclinic orbit at $\mu = 1/3$. However, if we further examine the speed of the increasing period with respect to the distance $(1/3 - \mu)$, it is much slower than the theoretical estimation $\frac{C}{(1/3 - \mu)}$ [7]. In fact, we found that there is a bound for such period: the maximal period for any periodic orbit that passes a small neighborhood of the origin is at the scale of $1/(0.01)^2 = 10000$. Our numerical results indicate that the maximal period is around 5000.

2. *Backward integration method:* The numerical estimation (13) gives us another way to verify the non-existence of homoclinic orbit by looking at the behavior of orbits close to the stable manifold when time $t \rightarrow -\infty$. First, it is easy to observe that all trajectories started in a neighborhood of the origin are bounded in positive time. We select a small ring (radius < 0.005) of initial points around the s -axis near the origin parallel to the $s = 0$ plane. When we integrate the system backward with these initial values, the stable manifold is located inside this cylindrical region. Our numerical result clearly shows that the stable manifold is escorted outside to infinity (see figure 2 (b)-(d)).

3.3. **Summary of numerical computations.** We summarize our numerical results on the dynamics and bifurcation of the system (2) with illustrations.

1. *The existence of homoclinic-like periodic orbits (figure 2 (a)):* For $\mu \in [1/3 - \delta, 1/3)$, and (α, β) in the region *I* in Figure 1, there is an attractive periodic orbit that resembles a homoclinic orbit. The period increases as $\mu \rightarrow 1/3$. The period also depends on parameters (α, β) . The period is the longest when $\mu \approx 0.333, \alpha = 2.5, \beta = 0.9$.

As μ approaches $1/3$ (when $\mu \geq 0.3331$), fewer orbits can be re-injected back towards the origin, many periodic orbits will stay inside the unstable manifold away from the origin. Orbits not very close to the unstable manifold near the origin can still be re-injected back towards the origin and stay in the unstable manifold thereafter (see Figures 3 (a) and (b)).

2. *The dynamics when $\mu = 1/3$:* At this Hopf-bifurcation point, almost no orbits started in a small neighborhood at the origin around the central manifold can leave the central manifold, which looks like a rather regular parabolic cone (Figure 3(c)). Some orbits outside can still be re-injected into this cone and it takes a very long time for them to spiral out (about 5000 time units). Then, the orbits form a limit cycle at the rim of the parabolic cone. No homoclinic-like periodic orbits are observed.

3. For the first type of the kinetic function $k_1(v)$, no homoclinic-like periodic orbits are found. There exists a sink not far from the origin and all the orbits started in a neighborhood of the origin are attracted to the sink. This reflects the fact that k_1 is closer to k_2 when (α, β) are small. When $\beta > 0$ is small: $\beta < 0.7$, there is also a sink which attracts orbits from the neighborhood of the origin.

4. *Periodic doubling in the supercritical region (Figures 4(a)-(i)):* A periodic doubling cascade in the supercritical region is not found for the kinetics k_1 , the size of the limit cycle increases without much change of its shape. A periodic doubling cascade of the limit cycle and an inverse cascade in the supercritical case for kinetics k_2 are found to occur when (α, β) is in region *II*, directly across the region *I* where homoclinic-like orbits occur.

4. BACK TO THE PDE MODEL

Further questions to be considered.

1. There exists numerical evidence that Hopf-bifurcation exists for the PDE system [4]. Does the classification of Hopf bifurcation apply to the PDE system too? i.e, in the region *I*, is the Hopf-bifurcation subcritical?

2. Is there a homoclinic orbit in the PDE system?

3. As we vary parameters $\mu, \alpha,$ and β with respect to time t , can we obtain solutions with irregular intermittent burstings (see Fig. 5)?

4. Does the pseudo-spectral approximation apply to the two phase solid combustion model [10] [12] [13] If it does, do we obtain similar dynamics for the finite dimensional system?
5. This 3D model is obtained by projecting the PDE system onto a 4 dimensional space. Do we obtain subtle changes of the dynamics when we increase the dimension of the space (increase the number of modes)?

REFERENCES

- [1] M. L. Frankel, G. Kovacic, V. Roytburd, and I. Timofeyev, Finite-dimensional dynamical system modeling thermal instability, 1997 preprint.
- [2] M. L. Frankel and V. Roytburd, A free boundary problem modeling thermal instabilities: well-posedness, *SIAM J. Math. Anal.* Vol 25, No 5, 1357-1374
- [3] M. L. Frankel and V. Roytburd, A free boundary problem modeling thermal instabilities: Stability and Bifurcation, *J. Dynamics and Differential Equations*, Vol. 6, No. 3, 1994
- [4] M. L. Frankel and V. Roytburd, Dynamical portrait of a model of thermal instability, cascades, chaos, reversed cascades and infinite period bifurcations, *International Journal of Bifurcation and Chaos*, Vol. 4, No. 3, (1994)
- [5] M. L. Frankel and V. Roytburd, Finite-dimensional model of thermal instability, *Appl. Math. Lett.* Vol. 8, No. 2, 39-44, 1995
- [6] J. Guckenheimer and P. Holmes, Nonlinear Oscillations, Dynamical Systems, and Bifurcations of Vector Fields, Springer-Verlag, 1983
- [7] J. Guckenheimer and A. R. Williams, Analysis of a subcritical Hopf-homoclinic bifurcation Preprint 1998
- [8] Po Deng and K. Saitamoto, Slinikov-Hopf bifurcation, *J. Differential Equations* 119, 1-23, 1995
- [9] X. Lin, Using Melnikov's method to solve Slinikov's problems, *Proc. of the Royal Society of Edinburgh*, 116A, 295-325, 1990
- [10] I. Brallovsky and G. Sivashinsky, Chaotic dynamics in solid fuel combustion, *Physics D* 65 (1993) 191-198
- [11] M. Bosch and C. Simo, Attractors in a Slinikov-Hopf scenario and a related one-dimensional map, *Physics D* 62 (1993) 217-229
- [12] S-N, Chow and W. X. Shen, A free boundary problem related to condensed two-phase combustion. I. Semigroup. *J. Differential Equations* 108 (1994), no. 2, 342-389.
- [13] S-N, Chow and W. X. Shen, A free boundary problem related to condensed two-phase combustion. II. Stability and bifurcation. *J. Differential Equations* 108 (1994), no. 2, 390-423
- [14] P. Hirschberg and E. Knobloch, Slinikov-Hopf Bifurcation, *Physics D* 62 (1993) 202-216

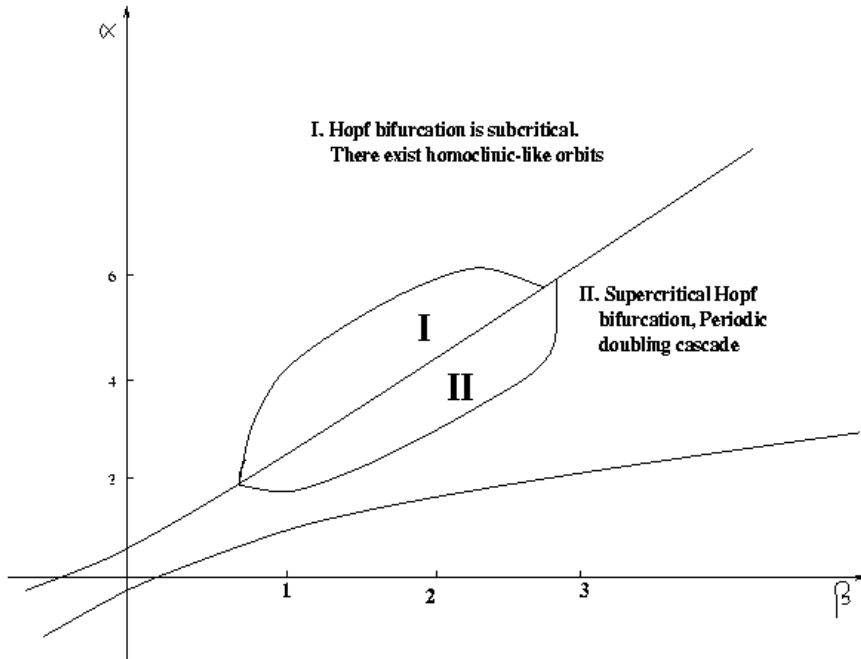


FIGURE 1. Bifurcation diagram for the Hopf bifurcation point $\mu = 1/3$ of the second type kinetic function $k_2(v)$

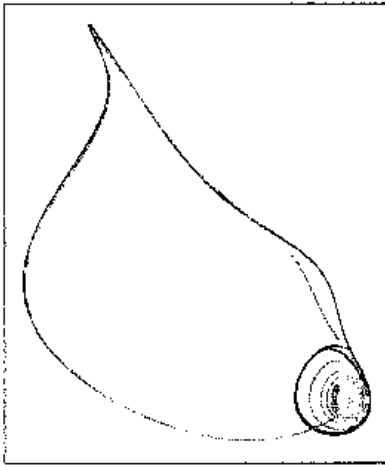


Fig. 2 (a) 'Homoclinic-like' orbits

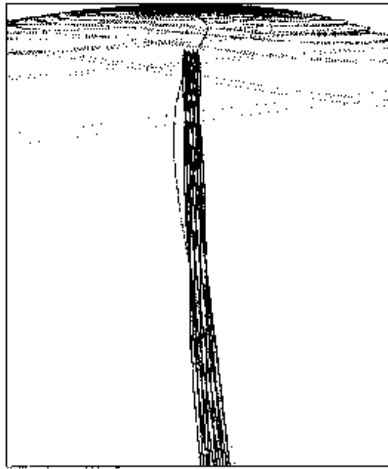


Fig. 2 (b) Stable manifold escorted out of the neighborhood of the equilibrium

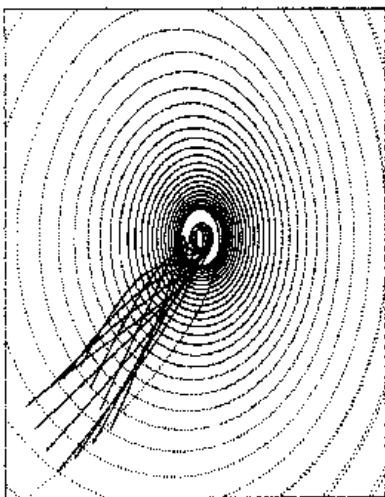


Fig. 2 (c) Inside the parabolic cone

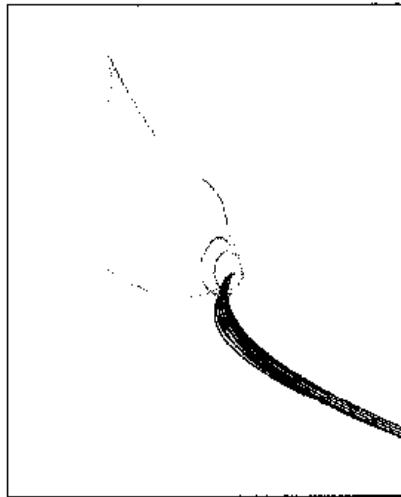


Fig. 2 (d) Stable manifold goes to infinity

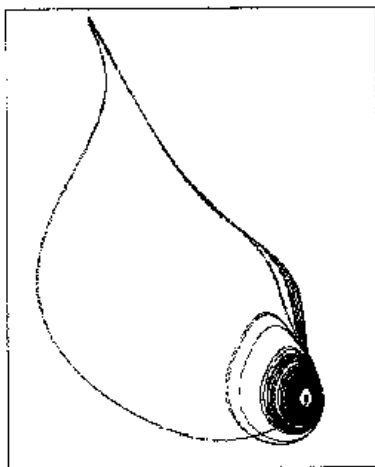


Fig. 3 (a) Orbits leave the neighborhood of the equilibrium and re-enter it. $\mu=0.33$

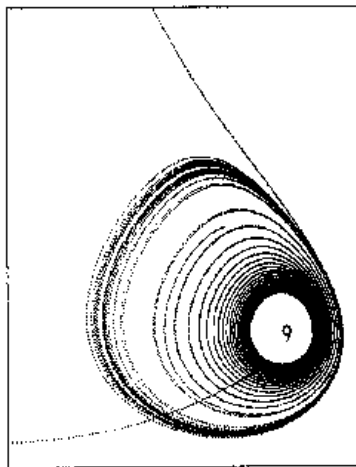


Fig. 3 (b) Fewer orbits can leave the neighborhood as μ approaches $1/3$, e.g., $\mu=0.3331$

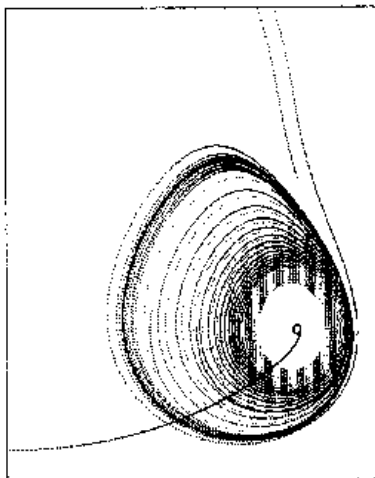


Fig. 3 (c) When $\mu=1/3$, only orbits rather far away from the origin can be re-injected back and stay in the parabolic cone.

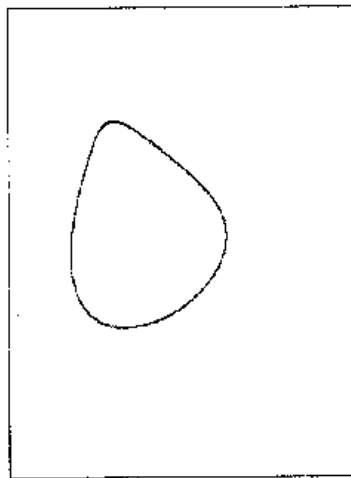


Fig. 4 (a) A limit cycle when (α, β) is in region II and μ is close to $1/3$; $\mu=0.33$.

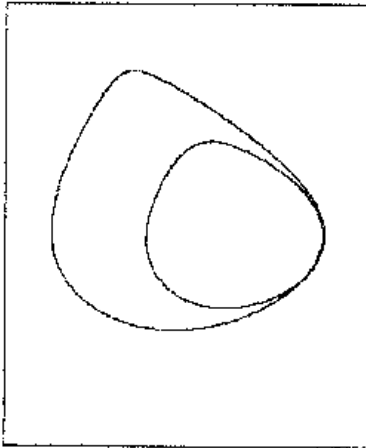


Fig.4 (b) Limit circle doubles its period as μ decreases: $\mu=0.327$.

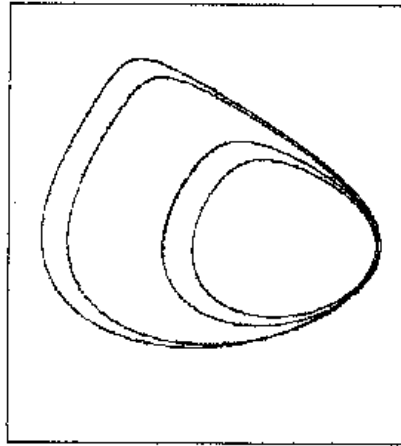


Fig. 4 (c) Period doubles to 4. $\mu=0.3267$.

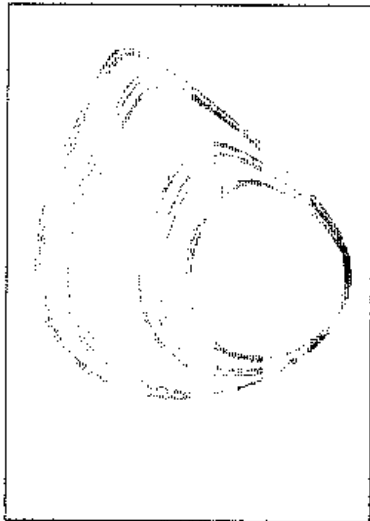


Fig.4 (d) $\mu= 0.3265$

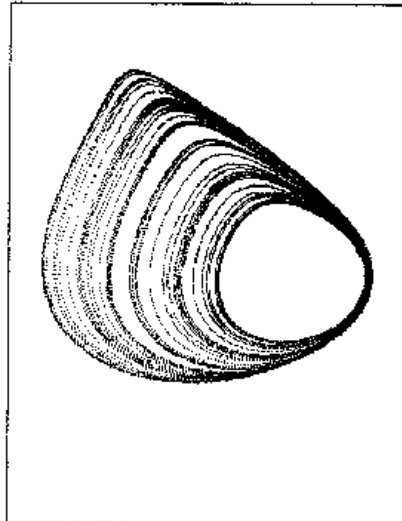


Fig.4 (e) $\mu=0.3263$

The Inverse Cascade of Periodic Doubling

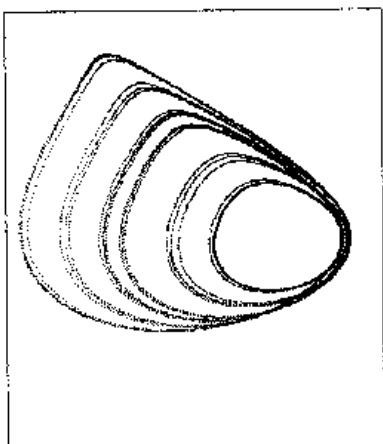
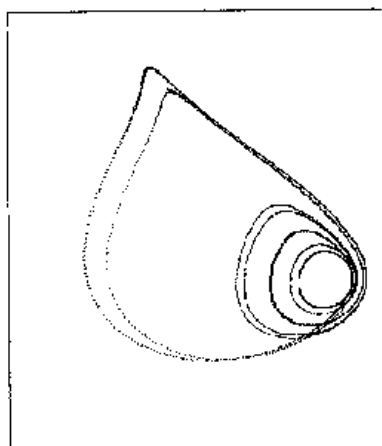
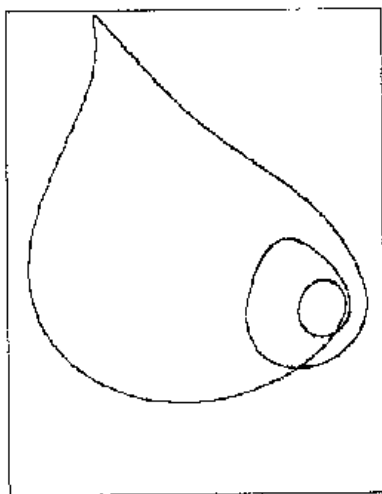
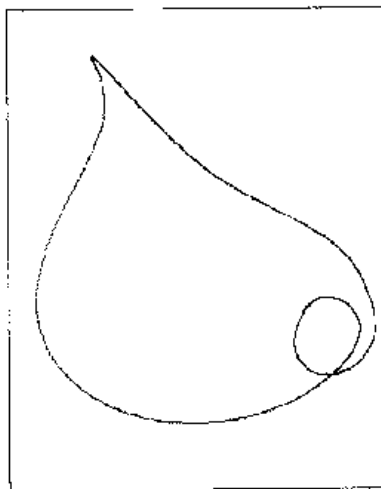
Fig.4 (f) $\mu=0.326$ Fig.4 (g) $\mu=0.324$ Fig.4 (h) $\mu=0.32$ Fig.4 (i) $\mu=0.31$

FIGURE 2. (a) 'Homoclinic-like' orbits; (b) Stable manifold escorted out of the neighborhood of the equilibrium; (c) Inside the parabolic cone; (d) Stable manifold goes to infinity.

FIGURE 3. (a) Orbits leaving the neighborhood of the equilibrium and re-entering it $\mu = 0.33$; (b) Fewer orbits can leave the neighborhood as μ approaches $1/3$: $\mu = 0.3331$; (c) When $\mu = 1/3$, only orbits started rather far away from the origin can be re-injected back and stay in the parabolic cone.

FIGURE 4. (a) A limit cycle when $(\alpha, \beta) = (2, 0.9)$ and $\mu = 0.33$; (b) Limit cycle doubles its period as μ decreases: $\mu = 0.327$; (c) Period doubles to 4. $\mu = 0.3267$; (d) $\mu = 0.3265$; (e) $\mu = 0.3263$; (f) $\mu = 0.326$; (g) $\mu = 0.324$; (h) $\mu = 0.32$; (i) $\mu = 0.31$

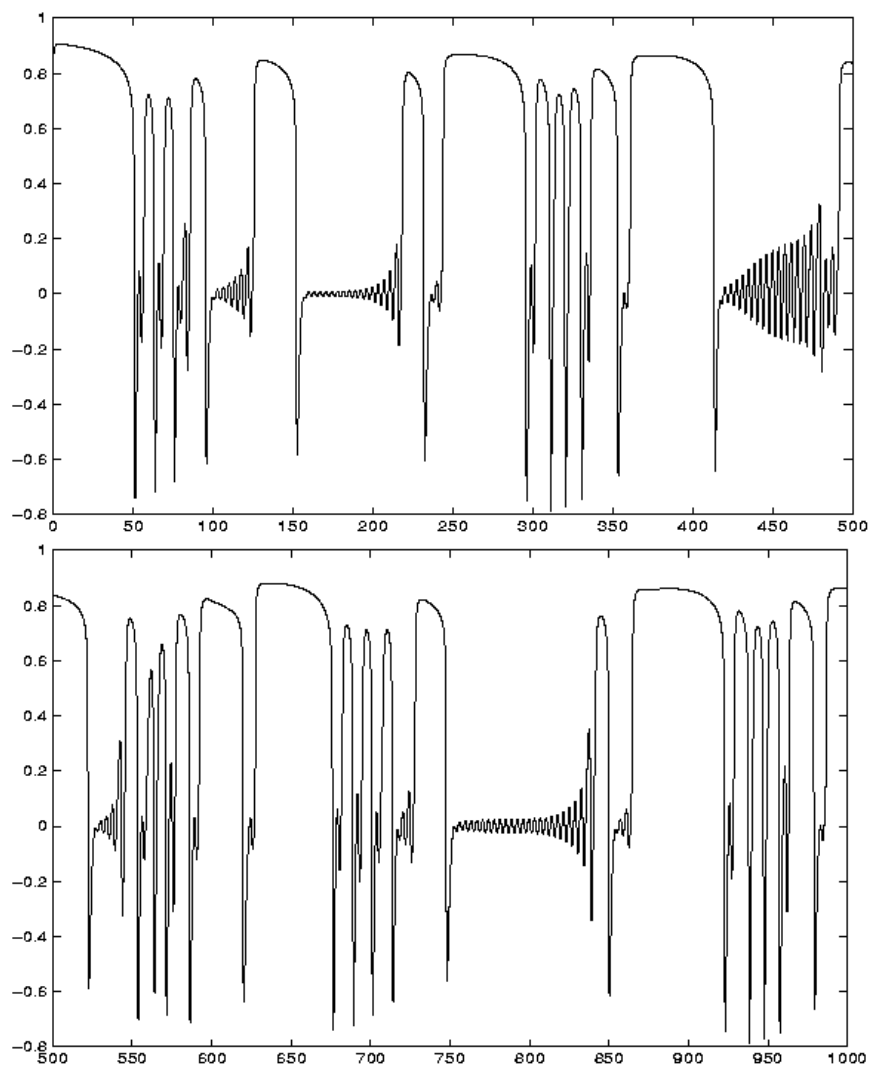


FIGURE 5. Intermittency ?